Integrative and Comparative Biology

Integrative and Comparative Biology, volume 61, number 2, pp. 414–426
https://doi.org/10.1093/icb/icab110

Society for Integrative and Comparative Biology

SYMPOSIUM

Foretelling the Flex—Vertebral Shape Predicts Behavior and Ecology of Fishes

Cassandra M. Donatelli[*,1], Alexus S. Roberts[†], Eric Scott[‡], Kylene DeSmith[‡], Dexter Summers[§], Layanne Abu-Bader[¶], Dana Baxter[‡], Emily M. Standen[*], Marianne E. Porter[||], Adam P. Summers[§] and Eric D. Tytell[‡]

[*]Department of Biology, University of Ottawa, Ottawa, ON K1N 6N5, Canada; [†]Department of Evolution and Ecology, University of California Davis, Davis, CA 95616, USA; [‡]Department of Biology, Tufts University, Medford, MA 02155, USA; [§]Department of Organismic and Evolutionary Biology, Harvard University, Cambridge, MA 02138, USA; [¶]Biology and SAFS, Friday Harbor Labs, University of Washington, WA 98250, USA; [||]Department of Biology, Florida Atlantic University, Boca Raton, FL 33431, USA

From the symposium "An evolutionary tail: Evo-Devo, structure, and function of post-anal appendages" presented at the virtual annual meeting of the Society for Integrative and Comparative Biology, January 3–7, 2021.

[1]E-mail: cassandra.donatelli@gmail.com

Synopsis One key evolutionary innovation that separates vertebrates from invertebrates is the notochord, a central element that provides the stiffness needed for powerful movements. Later, the notochord was further stiffened by the vertebrae, cartilaginous, and bony elements, surrounding the notochord. The ancestral notochord is retained in modern vertebrates as intervertebral material, but we know little about its mechanical interactions with surrounding vertebrae. In this study, the internal shape of the vertebrae—where this material is found—was quantified in 16 species of fishes with various body shapes, swimming modes, and habitats. We used micro-computed tomography to measure the internal shape. We then created and mechanically tested physical models of intervertebral joints. We also mechanically tested actual vertebrae of five species. Material testing shows that internal morphology of the centrum significantly affects bending and torsional stiffness. Finally, we performed swimming trials to gather kinematic data. Combining these data, we created a model that uses internal vertebral morphology to make predictions about swimming kinematics and mechanics. We used linear discriminant analysis (LDA) to assess the relationship between vertebral shape and our categorical traits. The analysis revealed that internal vertebral morphology is sufficient to predict habitat, body shape, and swimming mode in our fishes. This model can also be used to make predictions about swimming in fishes not easily studied in the laboratory, such as deep sea and extinct species, allowing the development of hypotheses about their natural behavior.

Introduction

One of the key evolutionary innovations that separates vertebrates from invertebrates is the notochord, a central element that provides the stiffness needed for fast and powerful locomotion (Symmons 1979; Long 1995; Koehl et al. 2000; Long et al. 2002; Annona et al. 2015). Later in evolutionary history, the notochord was mostly replaced by segmented vertebrae, though it is still present in all vertebrates (Annona et al. 2015). In bony fishes, the extent to which the notochord is present varies. In some fish, it simply makes up the intervertebral material. In others, it is the main structural component of the vertebral column and is present as a continuous tube running through the center of sometimes poorly mineralized vertebral centra. Because the vertebral column is important for swimming mechanics, it has been examined in several capacities to assess how anatomical variations impact the mechanics of fish swimming with one of the most commonly measured variables being bending stiffness. Studies of

Advance Access publication June 28, 2021

vertebral column bending stiffness have looked at single joints (Hebrank et al. 1990; Long 1991, 1995; Long et al. 1997; Nowroozi et al. 2012), as well as the entire vertebral column (Long et al. 2002; Porter et al. 2016). In this study, we build upon this literature by examining the functional effects of vertebral morphology, particularly the intervertebral elements (i.e., the notochord), as the relationship between these elements and swimming performance have not been systematically ! investig ated.

Most fishes with discrete vertebral centra exhibit similar morphological characteristics within the centra themselves (Schaeffer 1967; Larem 1975). Though the external body of a centrum (the central core) is cylindrical, the interior has two opposite facing cones oriented such that the wide ends are anteriorly and posteriorly directed, and the narrow ends meet in the middle to form a canal through the center (Fig. 1B–E). This results in an hourglass-like shape when a centrum is sectioned down the midsagittal plane (Fig. 1E). Attached to the dorsal and ventral sides of the main body of the centra are the neural and hemal spines, respectively. These spines start to appear on centra near the head and continue all the way to the caudal-peduncle. Neural spines are present on most vertebra, while hemal spines appear only after the cloaca. Anterior to the caudal-peduncle, the ribs protrude ventro-laterally and serve as protection for vital organs. Smaller and closer to the centra body are small interlocking spines called zygapophyses. These small spines vary greatly between species, but generally interlock adjacent centra along the length of the body (Liem et al. 2001).

Studies exploring the mechanical properties of the vertebral column and its anatomical components have resulted in many hypotheses about its role in swimming. Most of the work focusing on specific anatomy, like the intervertebral joints, has used larger swimmers such as the blue marlin (*Makaira nigricans*) (Hebrank et al. 1990; Long 1991) or the saddleback dolphin (*Delphinus delphis*) (Long et al. 1997), partially because it is methodologically easier to make mechanical measurements on larger species. These studies have revealed that, in both the saddleback dolphin and the blue marlin, the stiffness of the intervertebral joint increases from the cranium to about three quarters down the length of the body, and then decreases from that point to the caudal region (Aleyev 1977; Hebrank et al. 1990; Long 1991). Hebrank et al. (1990) also found that the zygapophyses in the blue marlin increase stiffness substantially when bending dorso-ventrally, but less so when bending laterally (Hebrank et al. 1990). In short, vertebral morphology varies within an animal, and this variation has a direct impact on the mechanical properties of individual intervertebral joints.

Regarding the vertebral column as a whole and its effect on swimming, Porter et al. (2016) found that the bending stiffness of the spiny dogfish (*Squalus sucklei*) vertebral column depended nonlinearly on frequency, suggesting that the vertebral column behaves as either a spring or a brake depending on swimming speed (Porter et al. 2016). Similarly, Long (1995), Long et al. (2002) determined that the mechanical properties of the hagfish (*Myxine glutinosa*) notochord, in conjunction with the body's musculature, help the animal adjust its resonant bending frequency for more efficient swimming; in the sturgeon (*Acipenser transmontanus*), notochord angular stiffness, not morphology, is inversely correlated with swimming kinematics (Long 1995; Long et al. 2002). Though these studies were mainly conducted on softer, more continuous structures, they reveal that the mechanics of the vertebral column is related to swimming performance.

In addition to the studies discussed above, there have been many more investigating the connection between swimming kinematics and the motion of the vertebral column, both as a whole and with a focus on individual intervertebral joints (Porter et al. 2009, 2014, 2016; Nowroozi and Brainerd 2014). In a meta-analysis of 20 different studies, spanning 28 species, Nowroozi and Brainerd (2014) found that the vertebral column experiences increasing degrees of bending from cranium to caudal region during steady swimming in undulatory swimmers. Though these observations do not directly discuss the shape or structural components of the vertebral column, we can use this information about undulatory locomotion in conjunction with more detailed morphological and mechanical studies to create models of locomotion in different species.

In addition to tests on biological specimens, physical models have played an important role in understanding the vertebral column (Hirokawa et al. 2011; Shelton et al. 2014; Lucas et al. 2015). Hirokawa et al. (2011) found that changing the morphology of a biomimetic vertebral column causes changes in the swimming speed and frequency of a bioinspired robot, MARMT (Hirokawa et al. 2011). Specifically, they found that decreased intervertebral joint length increases stiffness in a vertebral column inspired tail. In swimming flexible plastic foils, Lucas et al. (2015) found that foils with uniform stiffness swam more slowly than those with a stiffness gradient from anterior to posterior. This, along with Nowroozi and Brainerd's (2014) meta-analysis, suggests that the way the vertebral column changes from head to tail could affect swimming performance (Nowroozi and Brainerd 2014; Lucas et al. 2015). These studies also highlight the importance of using physical models to understand how individual morphological parameters affect swimming. By controlling for things

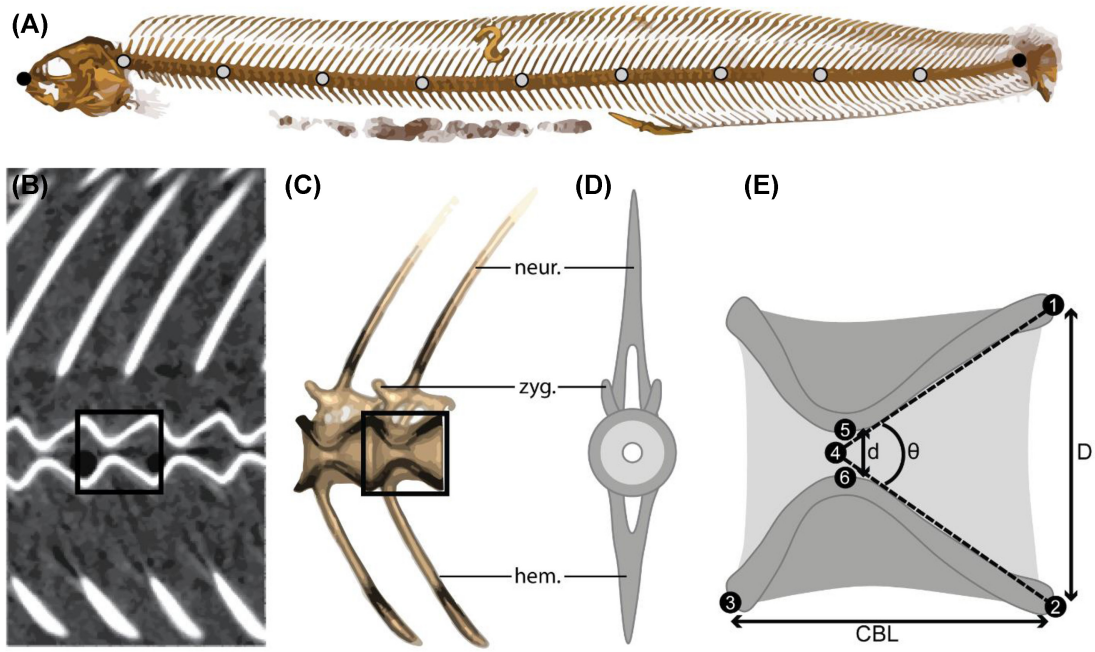

Fig. 1 Vertebral morphology measured in this study. (**A**) Lateral 3D rendering of one of our scanned specimens, *A. flavidus*, with the 10 evenly spaced points indicating where we took centrum measurements along the length of the body. (**B**) Single lateral slice through a selection of vertebrae generated with a micro-CT scanner. (**C**) Lateral 3D rendering of a pair of vertebrae. (**D**) Transverse diagram of a single vertebra showing the notochordal foramen in the center and select anatomy marked (neural spines—neur., zygapophyses—zyg., hemal spines—hem.). (**E**) Lateral diagram showing the points we used to calculate CBL, centrum diameter (*D*), centrum cone angle (θ), and centrum canal diameter (*d*).

such as material and individual variation, the results of studies using models can help us understand the links between specific aspects of internal vertebral morphology and swimming behavior.

Though many studies demonstrate that the mechanics of the vertebral column can have an important impact on swimming, very few of them have considered the internal shape of the vertebral centra and the role of the notochord. Because the notochordal material is much more flexible than the bony vertebrae, its properties may be more important in determining overall flexibility. Additionally, these studies have not examined multiple species to draw conclusions about how the common internal morphology of the vertebral column could relate to overall swimming behavior. In this study, we measured the vertebral morphology of 16 species of fishes with diverse body shapes that live in habitats ranging from intertidal to subtidal. To evaluate the functional role of the internal vertebral morphology, we used micro computed tomography to quantify the internal shape of the vertebrae. We then created and mechanically tested physical models of intervertebral joints with morphologies spanning the measured range. Next, we mechanically tested actual vertebral joints dissected from a subset of the species in this study. Finally, using the data from swimming trials performed on 13 species of fish, we created a statistical model that uses vertebral morphology to make predictions about the body shape, habitat, and swimming mode of these fishes.

Materials and methods

Swimming trials and kinematics

Study specimens

We collected individuals from 16 morphologically and ecologically diverse species of fish mostly native to the Salish Sea surrounding the San Juan Islands (Washington, USA). Specimens were collected using dip nets, beach seines, and otter trawls (Table 1) and then housed in sea tables connected to the flow through system at Friday Harbor Labs according to the University of Washington IACUC protocol 4238-03.

Swimming trials

We filmed fish swimming around a track in a modified sea table (Fig. 2). Once placed in the track, individuals were given time to adjust to the new tank and then allowed to swim around the track at their preferred steady swimming speed. We mounted a GoPro (GoPro Hero 5, GoPro, San Mateo, CA) above the tank to capture a dorsal view of the fish swimming through the

Table 1 Description of fish: short description of fishes used in this study

Genus	Species	Family	Habitat	Museum number
Anoplarchus	*insignis*	Stichaeidae	Intertidal	UW 157117
Ammodites	*personatus*	Ammodytidae	Nearshore	UW 157013
Apodichthys	*flavidus*	Pholidae	Nearshore	N/A
Anoplarchus	*purpurescens*	Stichaeidae	Intertidal	N/A
Aulorhynchus	*flavidus*	Aulorhynchidae	Nearshore	UW 006155
Cymatogaster	*aggregata*	Embiotocidae	Nearshore	N/A
Lepomis	*macrochirus*	Centrarchidae	Subtidal[a]	UW 119953
Lumpenus	*sagitta*	Stichaeidae	Subtidal	UW 044716
Myoxocephalus	*polyacanthocephalus*	Cottidae	Subtidal	UW 027606
Ophidon	*elongatus*	Hexagrammidae	Subtidal	N/A
Phytichthys	*chirus*	Stichaidae	Nearshore	N/A
Pholis	*laeta*	Pholidae	Nearshore	N/A
Pholis	*ornata*	Pholidae	Nearshore	N/A
Ronqulis	*jordani*	Bathymasteridae	Subtidal	UW 045926
Xiphister	*atropurpureus*	Stichaeidae	Intertidal	N/A
Xiphister	*mucosus*	Stichaeidae	Intertidal	N/A

[a]Lepomis *macrochirus* is a freshwater fish, so the "Habitat" description does not necessarily apply. We chose to identify it as "Subtidal" since it does not deal with the changing tides in its natural pond habitat.

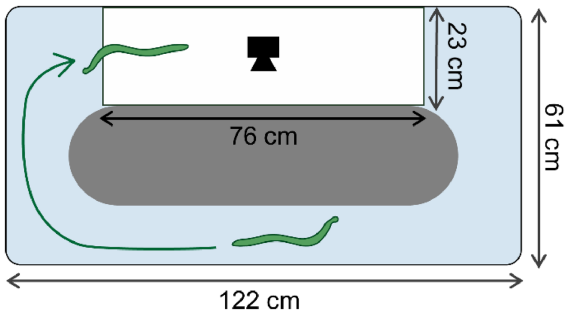

Fig. 2 Diagram of swimming track. The track was made in a modified sea table. Fish swam around the track until they were swimming at a consistent speed, then they were recorded with a GoPro in the filming area (white background).

filming area. For each species, we filmed five individuals swimming over several days until we had five steady swimming trials with at least five tailbeats per trial if possible. Because some fish could swim through the filming area in less than five tailbeats, we recorded more trials until we had a total of 25 tailbeats per fish.

Kinematic analysis

Video data were processed using custom Matlab code that traces the midlines of the fish in each frame of a swimming trial video and then uses the traces to extract kinematic parameters such as swimming speed (distance traveled in body lengths [BLs] per second), tail beat frequency (tail beats per second, Hz), tail beat amplitude (BL), and stride length (the distance traveled per tail beat, BL). For the purposes of this study, we only asked the code to output amplitude (Fig. 3). We also examined patterns of long-axis body twisting (wobble), in several elongate species used in this study. Wobble is a unitless ratio describing the amount of twisting where 0 is no twisting and 1 is body twisting of 90° (Donatelli et al. 2017; Fig. 3).

CT scanning and morphometrics

Study specimens

We collected morphological data from both museum and freshly fixed specimens representing 16 species of fishes. Individuals prepared for scanning were euthanized in a lethal dose (0.5 g/L) of MS222 according to the University of Washington IACUC protocol 4238-03 and stored in 70% ethanol for at least 24 h before scanning. For fish that were not available in the laboratory, we borrowed museum specimens from the Burke museum (Table 1) (Burke Museum of Natural History and Culture, Seattle, WA).

Scanning

All fishes were scanned at the Karel F. Liem Bio-Imaging Center at Friday Harbor Laboratories (Friday Harbor, WA, USA). Before scanning, we labeled specimens with radiopaque markers for easy identification during post-scan processing. Then, we wrapped multiple individuals in cheesecloth soaked in 70% ethanol and packed them into a 3D printed plastic tube. Once packed, we

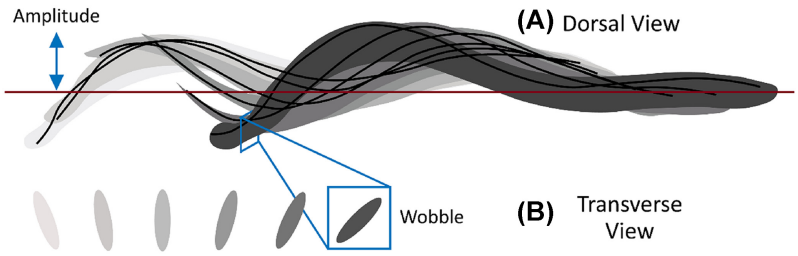

Fig. 3 Distance variables measured. (**A**) Dorsal view: Silhouettes of the body of *A. flavidus* swimming over several frames. Amplitude is the maximum distance the tail moves away from the axis of direction of motion (red line). (**B**) Transverse view: Wobble (W) is a ratio describing the magnitude of the torsional wave. In the transverse view, wobble is shown for the corresponding silhouettes in the dorsal view.

scanned the tubes using a Bruker Skyscan 1173 (Bruker, Belgium, Germany) at 65 kV and 123 µA with a voxel size ranging from 20.3 to 33.5 µm depending on the size of the specimens (higher resolution used for smaller specimens).

We reconstructed the scans using NRecon software by Bruker (2016, Bruker). Once reconstructed, the stacks were converted into nrrd files using ImageJ (Schneider et al. 2012) and imported into Slicer 3D (BWH and Contributors 2019). By examining nrrd files of each specimen in the three planes of traditional X-ray slices (Fig. 1B) as well as a 3D reconstruction of the fish (Fig. 1A and C) in Slicer 3D (BWH and Contributors 2019), we were able to collect morphometric data for each specimen. In total, we scanned and collected morphometric data from 48 specimens, with three specimens representing each of our 16 species.

Morphometrics

For each scanned specimen, we placed digital landmarks on multiple vertebrae along the length of the body in Slicer 3D. Vertebrae were selected at 10% BL intervals (Fig. 1A), resulting in morphometrics of eight to nine vertebrae sampled per individual. We placed six markers on each selected vertebra (Fig. 1E) and converted the coordinates to measurements in BL units. Markers 1, 2, 3, 5, and 6 were placed on physical landmarks of the centrum (Fig. 1E). Marker 4 was placed between markers 5 and 6 in the center of the notochordal foramen and was used as the apex to calculate centrum cone angle. We used measurements in terms of BL to correct for the difference in size of our study specimens. The resulting measurements gave us length of the vertebral centrum (CBL), diameter of the centrum's posterior facing cone (D), diameter of the centrum's central canal (d), and angle of the centrum's posterior facing cone (θ) (Fig. 1D). In addition to measuring the vertebral column, we also assigned each species a body shape, habitat, and swimming mode based on the literature and our own observations (Table 2; Lamb and Edgell 2010; Froese and Pauly 2019).

Once we collected centrum measurements in Slicer, we then used Matlab to calculate the ratio of soft to hard material in each vertebral centra. The area of the hard material (bone) was calculated using the area of a triangle made using points that defined centrum length (i.e., points 2 and 3; Fig. 1E), as well as one of the points that defined foramen diameter (i.e., point 6; Fig. 1E). We calculated the area of bone on both the dorsal and ventral side of the centra and summed the results to get "bone area." Similarly, the area of the soft material was calculated using the points that defined cone diameter (i.e., points 1 and 2; Fig. 1E), as well as the point that defined the center of the foramen (i.e., point 4; Fig. 1E). We did these calculations for both anterior and posterior centrum cones and summed the areas to get our "soft area" measurement. Once total areas were calculated, we divided the area occupied by soft material by the area occupied by bone to get the ratio of soft to hard material (S:H).

Material testing

Physical models

To investigate how the internal shape of vertebrae influences the mechanics of the vertebral joints, we made simplified and scaled up physical models of the centra of a representative subset of the species. We scaled the models up to roughly 20 times their natural size to work with them more easily and did not include the spines or zygapophyses. To minimize parameters tested, all models had the same external diameter and centrum length as well as a simplified cylindrical external structure (Fig. 4B). The parameters we chose to vary in the models were related to the shape of the internal hourglass-like structure, including centrum angle, diameter of the centrum cone, and canal diameter (Fig. 1A). We chose three different centrum angles (70°, 80°, and 90°), three different centrum cone diameters (15, 20, and 25 mm), and two different canal diameters (2 and 4 mm) to match the variation exhibited by specimens during preliminary data collection.

Table 2 Description of categories assigned to fish species

Body shape		**Habitat**	
Deep	High aspect ratio fishes	Pelagic	Spends most of their time in the water column
Fusiform	Low aspect ratio fishes with a torpedo shape	Sandy subtidal	Lives past the intertidal zone in sandy bottoms
Tadpole	Large head and quickly tapering body	Rocky subtidal	Lives past the intertidal zone in rocky or shale bottoms
Elongate	Longer than average body and a circular cross section	Nearshore	Follows the tide in and out, often living in eel grass or other plants
Laterally compressed	Long body and an extremely elliptical cross section	Sandy Intertidal	Lives in the sandy intertidal and often burrows under rocks
Eel-like	Extreme elongation (greater than 65 vertebrae) and an elliptical cross section	Rocky intertidal	Lives in the rocky intertidal
Swimming mode			
Pectoral	Swims mainly using their pectoral and/or pelvic fins		
Caudal	Swims mainly using the posterior one-third of their bodies; Carangiform swimming		
Body-caudal	Swims using the majority of their bodies; Anguilliform swimming		

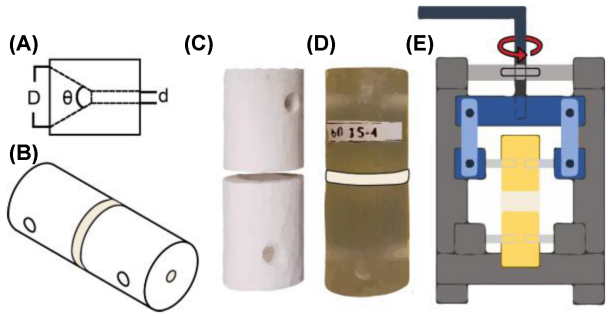

Fig. 4 Diagram of physical models and torsional rig. We designed the models to mimic the morphological variation found in vertebrae, varying centrum angle (θ), centrum diameter (D), and canal diameter (d) (**A**, **B**). For the first set of models, we 3D printed centra on a powder printer (**C**). Then, we aligned matching centra and cast them in PVC with Ecoflex to simulate intervertebral material. For the second set of models, we 3D printed them fully assembled with a multi-material 3D printer (**D**). Both sets of models were tested using a custom rig (**E**) connected to an Instron material testing system.

We created models of single vertebral joints (centra—intervertebral space—centra; Fig. 4) from two different sets of hard and soft materials to ensure that any variation we saw was due to shape, and not the material properties of the construction material. The first model centra were 3D printed on a powder printer (ZCorp 310; 3D Systems, MA) to simulate the bony vertebrae, with Ecoflex 00-10 (Smooth-On Inc., Macungie, PA, USA) cast in the gaps between the vertebrae (yellow region; Fig. 4B) to simulate the intervertebral material (Fig. 4C). For these models, we made three replicates of each different combination (e.g., 70° centrum angle, 15 mm centrum diameter, and 2 mm canal diameter) to account for variation in casting. The second set of models was printed fully assembled with a multi-material printer (Fig. 4D) (Connex Objet500; Stratasys Ltd., Eden Prairie, MN, USA). We used two materials: VeroClear for the centra and Tango+ for the intervertebral material, both of which are proprietary materials made by Stratasys specifically for their Connex printers. For the printed models, we used one replicate, as variation in printed models is 0.06% of model length with this system (Stratasys, 2018).

We measured the bending and torsional stiffness of the single joint models using an Instron material testing system (Instron, Norwood, MA, USA). Custom rigs held the models in place with pins (Fig. 4E) while each model was rotated or bent to a range of motion similar to or greater than what fish vertebrae would experience during steady swimming. We took the force displacement curves from the Instron and extracted the peak force for each trial using Matlab (Matlab R2018b, The MathWorks, Inc., MA, USA).

Real vertebral joints

We measured the maximum bending force before failure of a vertebral joint for a subset of the species in this study, including *Damalichthys vacca*, *Isopsetta isolepsis*, *Dasycottus setiger*, *Apodichthys flavidus*, and *Xiphister mucosus*. We chose these species because they are large, thus vertebrae were easier to dissect out and mount in the material testing system. Three individuals of each species were euthanized with a lethal dose (0.5 g/L) of MS222 according to the University of Washington IACUC protocol 4238-03. Once euthanized, we dissected out sections of the vertebral column containing four centra with the first centra being the one closest to the start of the anal fin. We chose to use four rather than two centra so that we could consistently grip

the small joints in our material testing system, though bending and failure occurred at only one joint (the joint between vertebrae 2 and 3 in this four-vertebrae prep). Once dissected out, we mounted vertebral sections in our material testing system with the anterior end being held stationary, and the other attached to the moving load cell. The load cell bent the samples laterally until the joint broke, and max load was recorded.

Statistical analysis

For the physical models, we performed a multiple regression analysis in R using the *Anova()* functions to determine how the parameters we varied affected torsional or bending stiffness (Fox and Weisberg 2019; R Core Team 2020). We tested each parameter individually, as well as the interaction between that parameter and the angle to which we twisted or bent the models.

We used a linear mixed effect model (lme4 package, *lmer()*) (Bates et al. 2015) to ask how vertebral morphology predicted swimming kinematics (bending amplitude and wobble) and mechanics (torsional modulus and torsional stiffness). Our predictors were the measurements we took of the vertebrae down the length of the body (Fig. 1E) with each row corresponding to a single vertebra. All measurements were scaled (*scale()*) to take into account the different orders of magnitude between linear measurements (centra length, centra diameter, and foramen diameter, in BLs) and angular measurements (anterior and posterior centra angle, in degrees). We included individual and species as random effects on the model intercept.

To more easily discuss the relationship between individual morphometric variables and position we created linear models using the *lm()* command in R to describe. In comparing linear, quadratic, and cubic models and for all morphometric variables, the best fit was quadratic (Fig. 5). We can then use coefficients from quadratic fits for each morphometric variable on each fish (intercept, slope, and quadratic coefficients of the equation $y = p_2x^2 + p_1x + I$) as descriptors of change along the body. These values will be represented with the tags "I," "p_1," and "p_2" where I represents the intercept of the line, p_1 represents the slope, and p_2 represents the curvature (i.e., the higher the p_2 value the more extreme the curve of the quadratic fit).

To ask how well morphology could predict categorical variables, we used linear discriminant analysis (LDA) (Martins 2014; Kassambara 2017). LDA is a method which uses the predictor variables (coefficients of the vertebral measurements down the length of the body in our case) to predict the class (body shape, swimming mode, or habitat) of an observation (species). We used the *lda()* function from the MASS package (Venables and Ripley 2002) in R to run each of our models, and quantified accuracy as the percentage of correct predictions from applying the model to test data (a subset of 15% of the total dataset). We created three models to test three different categorical variables relating to our data, including body shape, swimming mode, and habitat. For each of these models, our dependent variable was the category and the independent variables were the coefficients of our quadratic fit lines describing morphological and mechanical measurements along the length of the body. Each row of the matrix corresponded to one individual, with columns representing measurements at each point along the length of the body. We also used LDA to predict feeding habitat on a larger group of fishes (Froese and Pauly 2019). This larger group of fishes was primarily used for the tree visualization in the discussion, as that dataset only uses one individual from each species.

Results

Morphology

Overall, we found that vertebral morphology varies along the length of the body. Generally, vertebral measurements, with the exception of centrum length, increased from the cranium to around mid-body and then decreased from mid-body to caudal peduncle (Fig. 5). For most species and variables, the quadratic coefficient of the curve (p_2) was negative, meaning the measurements were at their maximum roughly 50% of the way down the length of the body. For some species and variables, the slope (p_1) was positive, or nearly zero.

Kinematics and mechanics

We found that some aspects of vertebral column morphology influenced swimming mechanics and kinematics (Table 3). For wobble, tail beat amplitude, torsional stiffness (GJ), and torsional modulus (G), at least some morphological variables were significant predictors (i.e., $P < 0.05$). Species means for kinematics and kinematics had high standard deviations due to variance along the body (supplementary Table S1). Our analysis including position accounted for this variation.

Material testing

For real fish joints, we found that as the ratio of soft material to bone (S:H) increased, the force to break the joint decreased ($P < 0.001$) (Fig. 6). For our models, we found that, as centrum diameter increased, both bending stiffness and torsional stiffness significantly decreased (Fig. 7 and Supplementary Table S2). The effects of centrum angle were nonlinear. For bending,

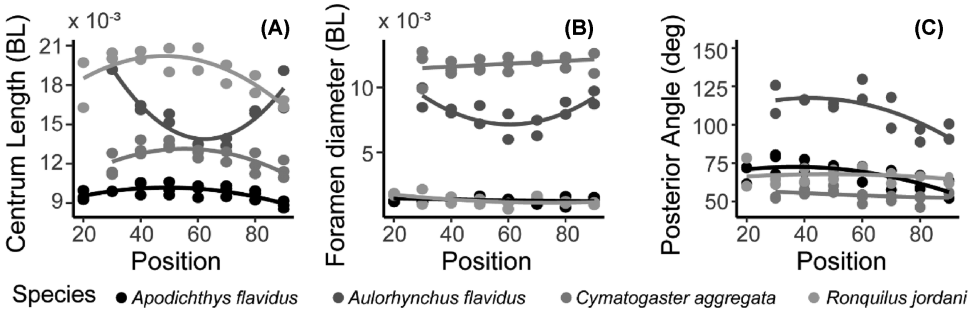

Fig. 5 Three of the six morphological parameters measured shown for 4 of 16 species. In the majority of our study species, CBL increases from anteriorly to posteriorly along the length of the fish until about 50% BL and then decreases posteriorly. A few species, including, *Au. flavidus* here, show an inverse trend (**A**). In contrast, most morphological variables, including foramen diameter and posterior cone angle (**B**, **C**), are relatively constant from head to tail. In most species, there is a peak at the midpoint of the body where the measurements reach their maximum or minimum values, though the prominence of that peak varies from species to species.

Table 3 LME results

	Wobble	Amplitude	GJ	G
Posterior diameter	0.113	**<0.001**	0.175	0.885
Anterior diameter	**<0.001**	0.320	0.517	0.390
Posterior angle	**0.083**	**<0.001**	0.087	0.621
Anterior angle	0.524	**<0.001**	**0.007**	**0.016**
Post diameter ∗ angle	0.870	0.968	0.860	0.706
Ant diameter ∗ angle	**<0.001**	0.660	0.720	**0.039**
Centra length	**0.144**	**<0.001**	**0.042**	0.943
Foramen diameter	**<0.001**	**0.004**	0.383	0.125

Numbers listed are *P*-values and highlighted values are where $P < 0.05$. Values are bolded when they represent a significant *P*-value ($P < 0.05$).

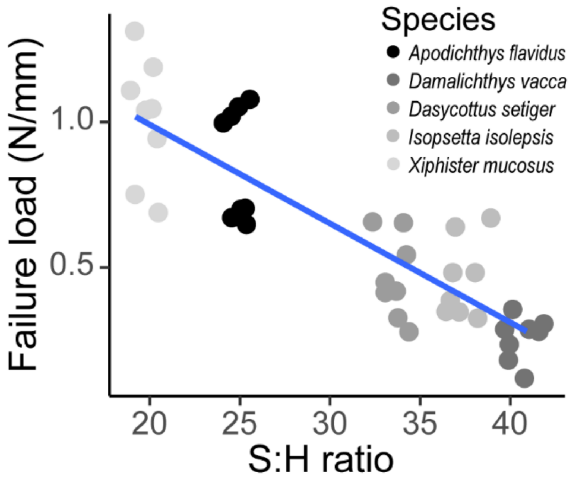

Fig. 6 Load to failure increases significantly ($P < 0.001$) as the amount of soft material in the vertebral centra decreases. S:H ratio is the ratio of the soft material in the centra to the bony material by area.

we observed peak stiffness in models with a centrum angle of 80°. There was a significant effect of bending angle on the Tango+ models ($P = 0.0043$), but not for the Ecoflex models ($P = 0.3632$). For twisting, there was a trough in stiffness with a centrum angle of 70° (Fig. 7). Similar to bending, twisting angle also had a significant effect on Tango+ models ($P = 0.0005$), but not Ecoflex models ($P = 0.6623$). Canal diameter did not have a significant effect on bending or torsional stiffness. The results from bending or twisting to 15° showed that the trends held for all angles of motion tested (Fig. 7). We chose to show the results of only the Tango+ models here, as the trends were more consistent (see Supplementary Table S1). The variation in Ecoflex models is likely due to manufacturing imperfections, as those were hand cast rather than printed as one unit.

LDA results

Our three LDA models showed significant separation between groups with different swimming modes, habitats, and body shapes (Table 4 and Fig. 8). The greatest predictive power was achieved when taking into account the centrum measurements taken along the length of the body (Fig. 1) and the calculated ratio of soft to hard material (Fig. 6). Loadings for each of the predictors can be found in Supplementary Table S3.

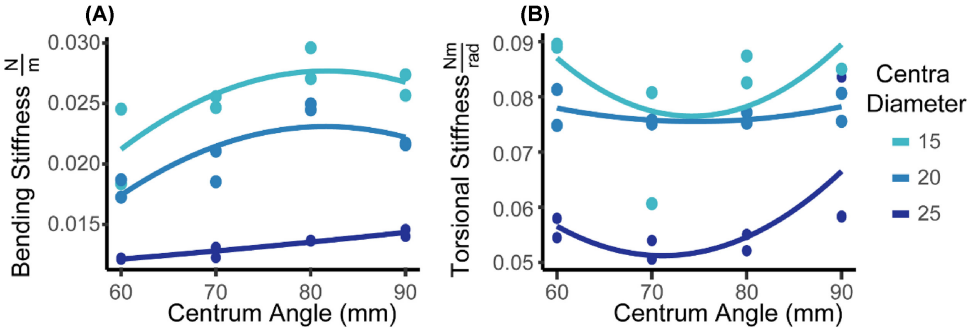

Fig. 7 Increases in centrum diameter result in decreases in both bending and torsional stiffness. Results from mechanical testing of Stratasys' printed models bent (**A**) and twisted (**B**) 15 degrees.

Table 4 LDA results

Model	Measurements along the body (C_M)			C_M + ratio of soft to hard material along the body		
Results	LD1	LD2	Accuracy	LD1	LD2	Accuracy
Mode	0.944	0.056	0.875	0.974	0.026	1.000
Habitat	0.588	0.189	0.833	0.640	0.140	1.000
Shape	0.419	0.247	1.000	0.432	0.292	1.000

LD1 and LD2 describe the amount of variance between groups described by that LD. Accuracy is the percentage of correct predictions made using the model and test data (a subset of 15% of the total dataset).

Discussion

This study has revealed that we can use vertebral morphology to predict the biology of 16 species of fishes. The degree of accuracy of our predictions varies, but it is often quite high (between 75–100%). Through our preliminary dataset of a larger variety of species, we have also shown that this method can be used to predict biology across the fish tree as well (Fig. 9) with functional components increasing the predictive power from 70% accuracy to 79% accuracy. Using functional testing of real vertebral joints and physical models, we showed that internal morphology of vertebrae can affect the mechanical properties of the intervertebral joints (Figs. 4 and 5), which may explain why these morphological parameters significantly predict swimming kinematics.

Fish vertebral morphology varies among species

Many aspects of vertebral morphology differ among species with one of the most variable traits being number of vertebrae, which can be as many as 260 in elongate species (Mehta et al. 2010) and as few as 28 in more fusiform shaped fishes (Yokogawa 2013) or even 16 in specialist species like ocean sunfish. In some species of fish, a greater number of vertebrae correlates with a greater curvature coefficient during C-starts (Brainerd and Patek 2016). Though we did not measure vertebral count directly, centrum BL (CBL) (Figs. 1E and 2A) can be used as a proxy since we measured it relative to the fish's BL. Our study species also differ in internal centrum morphology such as cone angle (alpha), cone diameter (D), and canal diameter (d). These species-specific differences in morphology correlate in a consistent way with body shape, habitat, and swimming mode (Fig. 8 and Supplementary Table S3). For example, by looking at the coefficients of our LDs, we can see that the slope (p_1) of CBL and anterior diameter along the body both contribute heavily to the separation between behavioral and body shape groups, though for habitat and shape, diameter p_1 is a greater contributor and, for swimming mode, diameter intercept (I) is a greater contributor. This could mean that there is a functional interaction between centrum length and anterior diameter that contributes to the overall shape and behavior of the fish. Generally, habitat and swimming mode have more highly contributing coefficients in common, such as the intercept of posterior cone angle and the intercept of the ratio of soft to hard material along the body.

These intervertebral morphological parameters have rarely been quantified, and our study represents the first time they have been measured and compared among multiple species. In particular, we have known about the notochordal foramen, which is the hole through the center of the vertebrae, from fossil species (Divay and

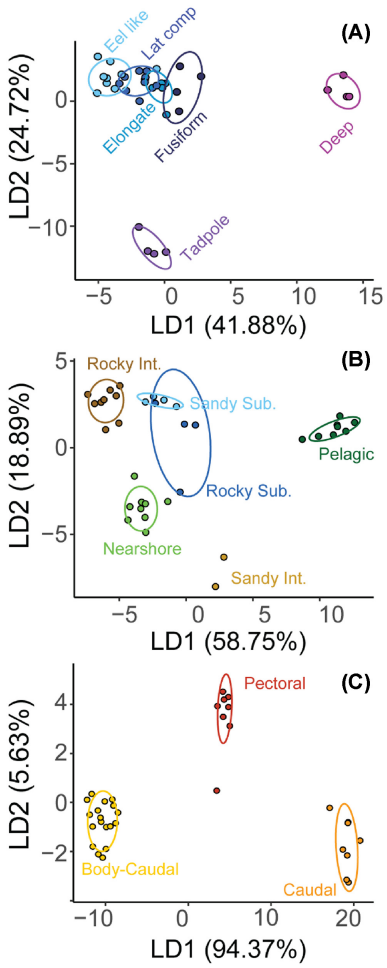

Fig. 8 Vertebral morphology can be used to predict attributes of fish biology. Percentages in axis labels are the percentage of between group variation described by that LD. Our LDA results show that the morphological variation in the vertebral column centra can be used to predict fish habitat (**A**), body shape (**B**), and swimming mode (**C**). Ellipses are drawn at a 95% confidence level using a multivariate *t*-distribution. No ellipse is drawn for "Sandy Intertidal" in B, as there are only two individuals in that category.

Murray 2013; Newbrey et al. 2013), but it has rarely been mentioned in extant species. Nowroozi et al. (2012) observed the foramen in the striped bass using histology. They noted that it may be possible for intervertebral fluid to flow through the canal, though it would take a great deal of pressure as the maximum diameter was 0.16 mm. In our study species, we observed the canal to be as wide as 1.1 mm, and we found canal diameter to be a significant predictor of both bending amplitude as well as wobble (Table 3). Perhaps the damping effect of the fluid flowing through differently sized foramen contributes to the steady swimming frequency fish choose as they bend and twist through the water. Future studies may employ fluid modeling to determine if and how fluid flow through the canal affects vertebral mechanics.

Vertebral morphology may be a proxy for other parameters

Using material testing, we showed that the internal vertebral morphology influences the mechanics of individual intervertebral joints in our printed models (Fig. 7) and several connected joints in real fish vertebrae (Fig. 6). Specifically, our physical models show that vertebrae with a smaller cone diameter are stiffer in both bending and torsion and real vertebrae show that more soft material in a joint means a lower force to break. When comparing morphology to swimming kinematics and mechanics of whole fishes, we found several parameters are significant predictors (Table 3). For example, CBL is a significant predictor of bending amplitude, wobble (body twisting), and torsional modulus and there are some interesting interactions to be explored involving anterior and posterior centra diameter and angle (Table 3).

Our study shows that the change in vertebral morphology down the length of the body is a significant predictor of a fish's preferred swimming mode. The most systematic study of the mechanics of intervertebral joints to date found variation in vertebral morphology down the length of the body in the striped bass (*Morone saxatilis*), similar to the variation we describe here (Nowroozi et al. 2012; Nowroozi and Brainerd 2014). This change in vertebral morphology, bending mechanics, and swimming kinematics down the length of the body has been observed in other species as well (Hebrank et al. 1990; Long 1991). Nowroozi observed that *M. saxatilis* do not laterally bend enough during swimming to reach the maximum possible bending angle of individual intervertebral joints (Nowroozi et al. 2012; Nowroozi and Brainerd 2014), though we show that a joint may not need to bend to max angle to have a significant effect on behavior. This could indicate a more complicated relationship between the internal morphology of the vertebral column, overall mechanics, and swimming.

Though internal measurements of the vertebral centra have generally been ignored when thinking about the mechanics of the system, we have shown they are as significant as centrum length in influencing mechanics (Table 3). Specifically, we have shown that including "functional" variables like ratio of soft to hard material in our LDA models increases predictive power (e.g., the ability of the model to predict categories like habitat). These functional variables may also link to other performance metrics. For example, in robotic

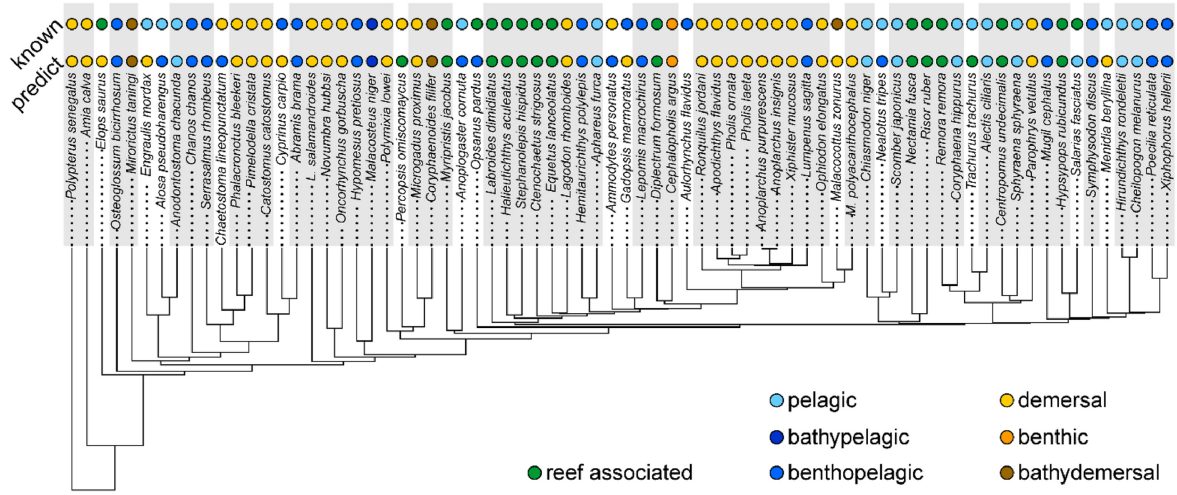

Fig. 9 Sample of predictive power of vertebral functional morphology based LDA models over a wider range of actinopterygian species. The top row of dots represents known habitat classifications and the bottom row represents predicted classifications. Correct predictions are highlighted in gray. Tree data were adapted from the fish tree of life database (Rabosky et al. 2018).

models, it has been shown that changing this ratio of hard to soft material decreases bending stiffness which leads to a decrease in both speed and acceleration during swimming (Hirokawa et al. 2011).

It is important to note that, while we have shown the relationship between intervertebral morphology and swimming kinematics to be strong, we recognize that no anatomical structures work in isolation. Our model allows us to accurately predict our biological classifications, but the morphology we measured may be proxies for other anatomical parameters that have a more significant effect. We did not include any measurement of neural and hemal spines, zygapophyses, or rib morphology, which can all affect how the vertebral column interacts with connective tissue (Hebrank et al. 1990). We also excluded parameters representing overall body shape, which can correlate with muscle mass and, thus, the stiffness down the length of the body during swimming (Wardle et al. 1995). Our focus on internal vertebral morphology provides insight on the impact of a centrum's stiff and flexible materials on swimming kinematics. However, this internal structure likely works in conjunction with the vertebral spines and connective tissues to influence the mechanics and kinematics of the vertebral column during locomotion.

Another interesting consideration is the material running through the notochordal foramen. As we mentioned earlier, in some species, the foramen is large enough that the notochord is still present as a continuous rod. In these species, the bony centra are quite thin and sometimes poorly mineralized. In this case, one might predict that the material properties of the notochord, instead of the bony joints, dominate the system. Our measurements of the internal centra diameter could also be a proxy for the shape of the notochord. It may be of use for future work to create physical models representing a continuous notochord to test whether bending and torsional stiffness change as the thickness of bony centra is varied.

Vertebral morphology is a reliable metric for predicting kinematics in fishes

Though the vertebral column is a small part of fish anatomy in terms of volume, we have shown that it provides reliable parameters for predicting the way various fish species live, likely due to its effect on the mechanics and function of the body. The vertebral column is the main structural component of a fish's body, providing attachment points for muscle and skin. Though studies have shown that connective tissue and muscle play a role in mechanics, our results demonstrate that the internal morphology of the vertebral column also significantly contributes to fish swimming mechanics. A few other studies on vertebral morphology also suggest that the difference in shape and number of vertebrae may affect the behavior of an animal. For example, when reef native eels are behaviorally constrained by their environment, they show a decrease in morphological variation (Mehta et al. 2010). In our data, a decrease in slope (p_1) or the quadratic coefficient (p_2) indicates a decrease in variation along the body. Perhaps these data could be used to predict behavioral adaptability in different behavioral and body shape groups.

We have shown that internal vertebral morphology can be used to predict the swimming kinematics of fishes from different habitats which have different body

shapes and swim using different modes. Models such as ours can also be used to make predictions about fish species for which we cannot collect kinematic data (Fig. 8). For example, it is very difficult to measure swimming kinematics for deep sea fishes and impossible to do so for extinct species. By comparing the vertebral morphology of such species with related and more easily accessible organisms, one can predict how other animals may move or may have moved in their natural environments. Finally, with the recent spike in freely available CT scans of fishes and other vertebrates, morphological data are becoming accessible for a huge variety of species (Cross 2017; Watkins-Colwell et al. 2018). We have shown that it is possible and very useful to describe how subtle variations in morphology play a significant role in locomotion.

Acknowledgments

The authors would like to thank Dr. Sarah Hoffman for help with testing the physical models. They would also like to acknowledge feedback from members of the 2018 and 2020 FHL fish courses as well as the 2020 REU-BLINKS program.

Funding

This work was supported by the following funding sources (NSF IOS 1652582, to E.D.T., and ARO grants W911NF-14-1-0268 and W911NF-17-1-0234 to E.D.T.; FHL Travel Fund, Tufts Grad Research Award, and 1852096 to C.M.D.; Center for Population Biology Travel Award, Graduate Students of Color Summer Research Award, NSF Graduate Research Fellowship under Grant No. 1650042 to A.S.R.; NSF 1759637 and 1701665 to A.P.S.; and NSF IOS 1941714 to M.E.P.).

Supplementary data

Supplementary data available at *ICB* online.

Data availability

The data underlying this article will be made available after proofs are finalized on GitHub at https://github.com/CDonatelli/FortellingTheFlex.

References

Aleyev YG. 1977. Nekton. Junk W, (ed.). The Hague: Publishers.

Annona G, Holland ND, D'Aniello S. 2015. Evolution of the notochord. EvoDevo 6:30.

Bates D, Maechler M, Bolker B, Walker S. 2015. Fitting linear mixed-effects models using lme4. J Stat Softw 67:1–48.

Brainerd EL, Patek SN. 2016. Vertebral column morphology, C-start curvature, and the evolution of mechanical defenses in tetraodontiform fishes. Copeia 1998:971–84.

BWH and Contributors. 2019. 3D Slicer.

Cross R. 2017. New 3D scanning campaign will reveal 20,000 animals in stunning detail. Sci News (doi: 10.1126/science.aap7604).

Divay JD, Murray AM. 2013. A mid-miocene ichthyofauna from the Wood Mountain Formation, Saskatchewan. Can J Vertebr Paleontol 33:1269–91.

Donatelli CM, Summers AP, Tytell ED. 2017. Long-axis twisting during locomotion of elongate fishes. J Exp Biol 220:3632–40.

Fox J, Weisberg S. 2019. An {R} companion to applied regression. 3rd edn. Thousand Oaks (CA): Sage.

Froese R, Pauly D. 2019. FishBase. World Wide Web Electronic Publication.

Hebrank JH, Hebrank MR, Long JH, Block BA, Wright SA. 1990. Backbone mechanics of the blue marlin *Makaira nigricans* (Pisces, Istiophoridae). J Exp Biol 148:449–59.

Hirokawa J, de Leeuw J, Krenitsky NM, Porter ME, Long JH, Roberts SF. 2011. Testing biomimetic structures in bioinspired robots: how vertebrae control the stiffness of the body and the behavior of fish-like swimmers. Integr Comp Biol 51:158–75.

Kassambara A. 2017. Machine learning essentials: practical guide in R. 1st edn. STHDA.

Koehl MAR, Quillin KJ, Pell CA. 2000. Mechanical design of fiber-wound hydraulic skeletons : the stiffening and straightening of embryonic notochords. Am Zool 40:28–41.

Lamb A, Edgell P. 2010. Coastal fishes of the Pacific Northwest. 2nd edn. Robson P, (ed.). Maderia Park (BC): Harbour Publishing.

Larem J. 1975. The development, function, and design of amphicoelous vertebrae in teleost fishes. Zool J Linn Soc 58:237–54.

Liem K, Bemis W, Walker WF, Grande L. 2001. Functional anatomy of the vertebrates: an evolutionary perspective. 3rd edn. Harcourt College Publishers.

Long JH. 1991. Stiffness and damping forces in the intervertebral joints of blue marlin (*Makaira nigricans*). J Exp Biol 155:131–55.

Long JH. 1995. Morphology, mechanics, and locomotion: the relation between the notochord and swimming motions in sturgeon. Environ Biol Fishes 44:199–211.

Long JH, Pabst DA, Shepherd WR, McLellan WA. 1997. Locomotor design of dolphin vertebral columns: Bending mechanics and morphology of *Delphinus delphis*. J Exp Biol 200:65–81.

Long JH, Koob-Emunds M, Sinwell B, Koob TJ. 2002. The notochord of hagfish *Myxine glutinosa*: visco-elastic properties and mechanical functions during steady swimming. J Exp Biol 205:3819–31.

Lucas KN, Thornycroft PJM, Gemmell BJ, Colin SP, Costello JH, Lauder GV. 2015. Effects of non-uniform stiffness on the swimming performance of a passively-flexing, fish-like foil model. Bioinspir Biomim 10:056019.

Martins TG. 2014. Computing and visualizing LDA in R (https://tgmstat.wordpress.com/2014/01/15/computing-and-visualizing-lda-in-r/).

Mehta RS, Ward AB, Alfaro ME, Wainwright PC. 2010. Elongation of the body in eels. Integr Comp Biol 50:1091–105.

Newbrey MG, Brinkman DB, Winkler DA, Freedman EA, Neuman AG, Fowler DW, Woodward HN. 2013. Teleost centrum and jaw elements from the Upper Cretaceous Nemegt

formation (Campanian–Maastrichtian) of Mongolia and a re-identification of the fish centrum found with the *Raptorex kreigsteini*. Divers Evol 291–303.

Nowroozi BN, Brainerd EL. 2014. Importance of mechanics and kinematics in determining the stiffness contribution of the vertebral column during body–caudal–fin swimming in fishes. Zoology 117:28–35.

Nowroozi BN, Harper CJ, De Kegel B, Adriaens D, Brainerd EL. 2012. Regional variation in morphology of vertebral centra and intervertebral joints in striped bass, *Morone saxatilis*. J Morphol 273:441–52.

Porter ME, Roque CM, Long JH. 2009. Turning maneuvers in sharks: predicting body curvature from axial morphology. J Morphol 270:954–65.

Porter ME, Diaz C, Sturm JJ, Grotmol S, Summers AP, Long JH. 2014. Built for speed: strain in the cartilaginous vertebral columns of sharks. Zoology 117:19–27.

Porter ME, Ewoldt RH, Long JH. 2016. Automatic control: The vertebral column of dogfish sharks behaves as a continuously variable transmission with smoothly shifting functions. J Exp Biol 219:2908–19.

Rabosky DL, Chang J, Title PO, Cowman PF, Sallan L, Friedman M, Kaschner K, Garilao C, Near TJ, Coll M, et al. 2018. An inverse latitudinal gradient in speciation rate for marine fishes. Nature 559:392–5.

Schaeffer B. 1967. Osteichthyan vertebrae. Zool J Linn Soc 47:185–95.

Schneider CA, Rasband WS, Eliceiri KW. 2012. NIH Image to ImageJ: 25 years of image analysis. Nat Methods 9: 671–5.

Shelton RM, Thornycroft PJM, Lauder GV. 2014. Undulatory locomotion of flexible foils as biomimetic models for understanding fish propulsion. J Exp Biol 217: 2110–20.

Symmons S. 1979. Notochordal and elastic components of the axial skeleton of fishes and their functions in locomotion. J Zool 189:157–206.

R Core Team. 2020. R: a language and environment for statistical computing. Vienna, Austria: R Foundation for Statistical Computing (https://www.R-project.org/).

Venables WN, Ripley BD. 2002. Modern applied statistics with S. 4th edn. New York: Springer US.

Wardle CS, Videler JJ, Altringham JD. 1995. Review tuning in to fish swimming waves: body form, swimming mode and muscle function. J Exp Biol 198: 1629–36.

Watkins-Colwell G, Love K, Randall Z, Boyer D, Winchester J, Stanley E, Blackburn D. 2018. The walking dead: status report, data workflow and best practices of the overt thematic collections network. Biodivers Inf Sci Stand 2: e26078.

Yokogawa K. 2013. Morphological variations in bluegill, *Lepomis macrochirus*, with particular emphasis on growth-related changes. Ichthyol Res 60:48–61.